Robotica (2010) volume 28, pp. 397–403. © Cambridge University Press 2009
doi:10.1017/S0263574709005712

Indoor localization system in a multi-block workspace

JaeHyun Park, MunGyu Choi, YunFei Zu and JangMyung Lee*

School of Electrical Engineering, Pusan National University, Pusan 609-735, Korea

(Received in Final Form: April 9, 2009. First published online: May 22, 2009)

SUMMARY

This paper proposes methodologies and techniques for multi-block navigation of an indoor localization system with active beacon sensors. As service robots and ubiquitous technology have evolved, there is an increasing need for autonomous indoor navigation of mobile robots. In a large number of indoor localization schemes, the absolute position estimation method, relying on navigation beacons or landmarks, has been widely used due to its low cost and high accuracy. However, few of these schemes have managed to expand the applications for use in complicated workspaces involving many rooms or blocks that cover a wide region, such as airports and stations. Since the precise and safe navigation of mobile robots in complicated workspaces is vital for the ubiquitous technology, it is necessary to develop a multi-block navigation scheme. This new design of an indoor localization system includes ultrasonic attenuation compensation, dilution of both the precision analysis and fault detection, and an isolation algorithm using redundant measurements. These ideas are implemented on actual mobile robot platforms and beacon sensors, and experimental results are presented to test and demonstrate the new methods.

KEYWORDS: Indoor localization; Multi-block navigation; Active beacon; Mobile robot.

1. Introduction

The problem of determining the location of a mobile robot in a room has been investigated in multiple ways over recent years. The relative positioning, such as dead reckoning (i.e., measuring the wheel rotation angles to compute the offset from a known starting position), is simple, inexpensive, and easy to implement in real time. However, this positioning has the problem of accumulating wheel slippage errors. The absolute positioning schemes are exemplified by the well-known satellite GPS system, in which the localization process is based on triangulation, using the distances between the GPS receiver on a mobile object, and three or more signal transmitters, i.e., satellites in the earth's coordinates. It is difficult to use GPS for indoor applications as this would be very expensive and would have the effect of shielding the signal. Some GPS-like indoor localization systems, such as ultrasonic positioning systems based on ultrasonic beacon sensors,[1,2] have been developed to provide absolute position information to the mobile robots. Some navigation methods, such as integrated ultrasonic localization and other relative positioning methods (e.g., inertial navigation or dead-reckoning navigation), can be utilized together[3,4,5] when more precise and extensive specifications are required. These integrated navigation systems are usually precise and reliable but can be expensive. These are useful in applications requiring precise manufacturing systems. In practice, the trade-off between accuracy and cost in a positioning system must be considered. This research focuses on maximizing the positioning accuracy at a relatively low cost. An active beacon system (ABS) is designed to achieve this goal, based on the beacon sensors providing the absolute position data to the indoor moving object.[6] The active beacon sensor consists of a radio frequency (RF) receiver and an ultrasonic transmitter mounted on the ceiling and walls of the room. A mobile robot can select a specific beacon, which has its own ID and position information during the navigation by sending a desired beacon code in RF. When a beacon receives its own ID from the robot, it sends back an ultrasonic signal to measure the distance from the beacon to the robot using the time-of-flight (TOF). The robot position can be computed by the triangulation method using the distances and the relative beacon position information.

An auto-calibration algorithm has been developed in order to deploy the ABS system in an easy and reliable manner.[7,8] The algorithm requires the user to set up several reference locations, known as seeds, on the floor. The system will collect a variety of distance data from the seeds to the beacons, which are installed on the wall without any position information. The position data for the beacons can be calculated, and stored in the beacons, by using the distance data from the seeds to the beacons. Note that the locations of the seeds are properly selected on the floor with prespecified position data.

As the service robot and the ubiquitous technology become more and more popular, the localization system could be deployed in complicated workspaces with multiple rooms and blocks. This paper proposes a multi-block navigation of the indoor ABS localization system.

2. Multi-Block Navigation

The localization of the mobile robot becomes extremely complex and difficult within a multi-block workspace. There are four problems to be solved in order to offer precise and flexible navigation. First, it is necessary to identify the space in which the robot is working. Second, the error in the TOF measurement becomes serious as the traveling distance of the ultrasonic signal increases in the multi-block workspace,

* Corresponding author. E-mail: jangmlee@hanmail.net

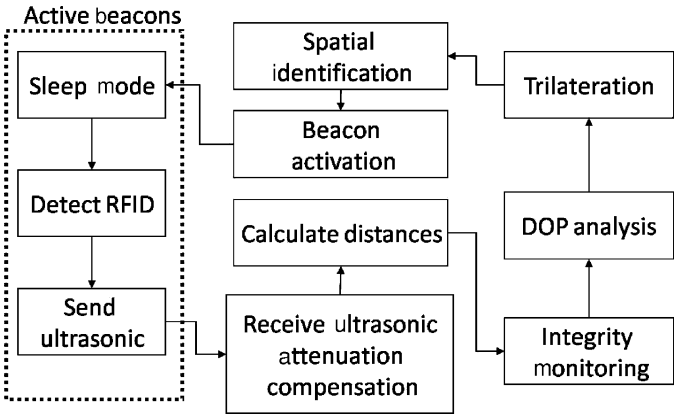

Fig. 1. The localization structure of the multi-block workspace.

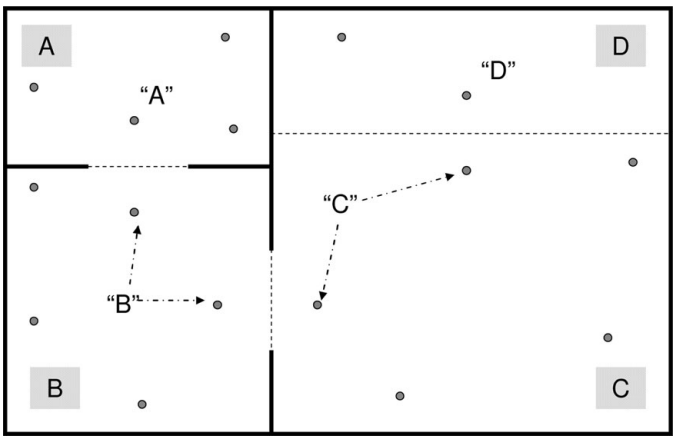

Fig. 2. Space ID (A, B, C, and D) and the beacons (circles).

which should be reduced to a certain level. Third, faulty beacons caused by equipment malfunction, such as ultrasonic echo, various interferences, or obstacles, should be detected and isolated from the normal signal. Fourth, it is necessary to select optimal beacons in individual and specific locations of the multi-block workspace when redundant beacons are available. That is, a method needs to be developed that chooses the minimum beacons necessary for the triangulation algorithm.

In order to solve these four problems, a new multi-block navigation system, based on the ABS system, is proposed in this paper. The structure of the multi-block navigation is shown in Fig. 1 where a spatial identification module is introduced to provide the space information to the robot. The space ID is obtained from the spatial identification, and the information for the relevant beacons is downloaded to the mobile object, which carries the localization system. The RFID transmitter in the localization system sends trigger signals to activate the relevant beacons. When the beacon receives its own ID, it sends an ultrasonic signal back to the mobile robot. The distance from the beacon to the mobile robot can be calculated by multiplying the TOF and travel speed of the ultrasonic signal. The error in this process can be compensated for by using an attenuation compensation module. Faulty beacons often result in fatal errors in the localization process and hence, a fault detection and isolation (FDI) algorithm, named Signal Integrity Monitoring, is proposed to eliminate it in the proposed method. Only healthy signals and highly reliable beacons are selected in order to precisely compute the robot position. The dilution of precision (DOP) analysis is implemented to determine which beacons can be used to obtain the most precise localization of the mobile robot if redundant measurements are still available after the fault detection and isolation. A sleep mode is also adopted for the active beacons, to save power while they are not in active use.

3. Spatial Identification

Since multi-block navigation is based on the ABS, range measurements need to be triggered by RFID signals, transmitted by the localization system on the mobile robot. A number of beacons are deployed in different areas (e.g., different rooms or floors) in the multi-block environment and the robot should be able to recognize which group of beacons is nearby and available for the localization.

A spatial identification method is proposed to provide the space ID, to identify in which block the mobile robot is located so that the system can trigger the relative beacons belonging to that block with its space ID. Figure 2 shows an example of the beacon deployment where there are three rooms in the workspace and there are four or more ceiling-mounted beacons deployed in each room. Notice that several couples of beacons can be placed at opposite sides of the mobile robot instantaneously, and which are at equal distances away from the space boundary; this may cause difficulties in selecting the most appropriate set of beacons for performing the robot localization. Each beacon has its own beacon ID, and it can also store the preset space ID. In some situations, a pair of beacons can be placed at equal distances away from the mobile robot, as is shown in Fig. 2. These couples of beacons must be handled carefully for precise localization in the navigation and localization process, since the space ID attached to the nearest beacon could be the current space ID. A pair of neighboring beacons may have a different space ID, demarcated by virtual space boundaries, which do not coincide with physical boundaries such as the walls. A space ID is assigned to a beacon heuristically while it is installed on the ceilings or the walls in this experiment for the sake of simplicity. Note that there are two space IDs, namely C and D, in the third large room.

4. Attenuation Compensation

Attenuation is the reduction in the amplitude and intensity of a signal. Signals may be attenuated exponentially by transmission through a medium, in which case attenuation is usually reported in dB with respect to the distance traveled through the medium. Attenuation can also be understood as being the opposite of amplification. Attenuation is an important property in telecommunications and ultrasound applications as the signal strength can be a key factor in distance measurement. The TOF measurement process and attenuation effect is illustrated in Fig. 3. When a beacon receives the RFID signal with its own ID from the robot, it sends back an ultrasonic signal. The localizer checks the arrival of the ultrasonic signal, and measures

https://doi.org/10.1017/S0263574709005712 Published online by Cambridge University Press

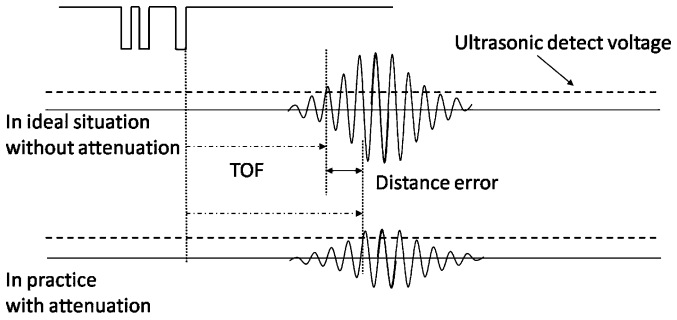

Fig. 3. Illustration of the TOF measurement.

the TOF, simultaneously by counting pulses. When the counter stops the TOF is obtained when the amplitude of the ultrasonic signal is bigger than a threshold value determined heuristically. However, as the distance from the beacon to the robot increases in the multi-block workspace compared with a simple space, the amplitude of the ultrasonic can be greatly attenuated. The TOF measurement becomes prone to error if the same threshold value for the near beacon is used for detecting the arrival of the ultrasonic signal.

This paper proposes an attenuation compensation algorithm in order to decrease the TOF errors. In this algorithm, a variable threshold voltage is defined as

$$V = V_0 - A_0 e^{-ax}, \tag{1}$$

where A_0 is the amplitude of the propagating wave at a reference location where $x = 0$, V_0 is the received voltage of the ultrasonic signal at A_0, and a is a positive attenuation coefficient, which can be determined by the status of the traveling path. The amplitude $A_0 e^{-ax}$ is the reduced amplitude after the wave has traveled a distance x from the reference location. The initial threshold value is set as the reference location, which is the nearest location of the mobile robot from the beacon. This location could be directly below the beacon when the beacons are attached normally on the ceilings. By using the initial threshold value, V_0, the distance is measured as x. The new threshold value is determined, and used to compensate for the attenuation by using Eq. (1).

5. Dilution of Precision

The performance of the triangulation algorithm is affected by the ranging errors, by the geometrical arrangement of the beacons, and by the location of the mobile robot. The geometry causes the DOP effect, i.e., the ranging error is amplified while the position vector is computed.

Assume that the range measurement errors are uncorrelated with the same variance σ^2. Then the definition of the geometric DOP [9] is given as

$$\text{GDOP} = \frac{\sqrt{\sigma_x^2 + \sigma_y^2 + \sigma_z^2}}{\sigma}, \tag{2}$$

where σ_x^2, σ_y^2, and σ_z^2 are the x, y, and z directional variances, respectively. The measurement error equation, in the three-dimensional space, for each beacon with known coordinates (x_i, y_i, z_i) and unknown user coordinates (X, Y, Z), is given by

$$\rho^i = \sqrt{(x_i - X)^2 + (y_i - Y)^2 + (z_i - Z)^2} \tag{3}$$

where ρ^i represents the measurement error at (x_i, y_i, z_i). This nonlinear equation can be linearized by using a Taylor series expansion.[9]

The basic measurement relationship of the triangulation method can be represented as

$$y = \mathbf{H}x + \upsilon_\rho, \tag{4}$$

where the additive white noise, with variance σ^2, is denoted as $\upsilon_\rho \in N(0, \sigma^2)$, y represents the difference between the actual measured range and the predicted range, based on the nominal user position, x is a 3×1 vector for the true position deviation from the nominal position, and $\mathbf{H}$ is the usual linear connection matrix obtained by linearizing the nominal user position.

The least squares solution can be obtained as[10]

$$\hat{x} = (\mathbf{H}^T \mathbf{H})^{-1} \mathbf{H}\, y. \tag{5}$$

Now, the error covariance is represented as

$$E\left\langle (\hat{\mathbf{x}})(\hat{\mathbf{x}})^T \right\rangle = \sigma^2 (H^T H)^{-1}. \tag{6}$$

For $\hat{\mathbf{x}} = [\Delta X\ \Delta Y\ \Delta Z]^{-1}$,

$$E\langle \hat{\mathbf{x}}(\hat{\mathbf{x}})^T \rangle = \begin{bmatrix} E\langle \Delta X^2 \rangle & E\langle \Delta X \Delta Y \rangle & E\langle \Delta X \Delta Z \rangle \\ E\langle \Delta Y \Delta X \rangle & E\langle \Delta Y^2 \rangle & E\langle \Delta Y \Delta Z \rangle \\ E\langle \Delta Z \Delta X \rangle & E\langle \Delta Z \Delta Y \rangle & E\langle \Delta Z^2 \rangle \end{bmatrix}. \tag{7}$$

From the properties of the linear connection matrix, it is necessary to only focus on the diagonal elements of

$$(H^T H)^{-1} = \begin{bmatrix} A_{11} & A_{12} & A_{13} \\ A_{21} & A_{22} & A_{23} \\ A_{31} & A_{32} & A_{33} \end{bmatrix}. \tag{8}$$

From the GDOP definition, this is obtained as

$$GDOP = \sqrt{A_{11} + A_{22} + A_{33}}, \tag{9}$$

which can be utilized to evaluate the beacon reliability, where the best reliable beacon has the lowest GDOP value.

6. Signal Integrity Monitoring

Signal integrity monitoring is proposed for multi-block navigation, based on the ABS system. The basic principle is to use the redundant TOF measurements to detect and exclude any faulty beacons. To obtain a three-dimensional position of the mobile robot, at least three measurements from the beacons to the robot are required. To detect a fault, at least four measurements are required, and when there are more than four measurements available, it is possible to isolate and exclude a faulty beacon.

https://doi.org/10.1017/S0263574709005712 Published online by Cambridge University Press

The QR factorization decomposition of the $n \times 3$ matrix $\mathbf{H}$ is[11]

$$\mathbf{H}_{n\times 3} = \mathbf{Q}_{n\times n}\begin{bmatrix}\mathbf{R}_{3\times 3}\\ \mathbf{0}_{(n-3)\times 3}\end{bmatrix}, \tag{10}$$

where $\mathbf{Q}_{n\times n}$ is an orthogonal matrix satisfying $\mathbf{Q}^T\mathbf{Q} = \mathbf{I}$, $\mathbf{R}_{3\times 3}$ is an upper triangular matrix, and $\mathbf{0}_{(n-3)\times 3}$ is a null matrix. Premultiplying both sides of Eq. (9) by $\mathbf{Q}^T$ will result in

$$\mathbf{Q}^T\mathbf{H}_{n\times 3} = \mathbf{Q}^T\mathbf{Q}_{n\times n}\begin{bmatrix}\mathbf{R}_{3\times 3}\\ \mathbf{0}_{(n-3)\times 3}\end{bmatrix} = \begin{bmatrix}\mathbf{R}_{3\times 3}\\ \mathbf{0}_{(n-3)\times 3}\end{bmatrix}. \tag{11}$$

The parity matrix $\mathbf{P}$ is defined to satisfy $\mathbf{P}\,\mathbf{H} = 0$, and is actually

$$\mathbf{P} = \textbf{bottom} \quad (n-3) \quad \textbf{rows of} \quad \mathbf{Q}^T. \tag{12}$$

The parity vector p is also defined as $p = \mathbf{P}y$[12]. That is,

$$p = \mathbf{P}y = \mathbf{P}\left(\mathbf{H}x + \upsilon_\rho\right) = \mathbf{P}\upsilon_\rho. \tag{13}$$

A signal risk factor F_S is defined and used for the test statistics:

$$F_S = p^T p. \tag{14}$$

Based on this signal risk factor, the probability of a faulty measurement can be expressed by the following equation:[13,14]

$$P_{MD} = P\left(F_S < \mathrm{T_S} \mid \text{fault occurred}\right). \tag{15}$$

The value of a threshold T_S could be determined for the probabilities of a faulty measurement, based on the user's requirement. A fault detection warning will be displayed on the user interface when the test statistic of the signal risk factor exceeds the threshold.

In the presence of a bias fault $\mathbf{b}$, the measurement of Eq. (4) becomes

$$y = \mathbf{H}x + \mathbf{b} + \upsilon_\rho. \tag{16}$$

Assuming that the ith measurement is faulty,

$$\mathbf{b} = \begin{bmatrix}0 & \cdots & b_i & \cdots & 0\end{bmatrix}^T. \tag{17}$$

Substituting Eqs. (16) and (17) into Eq. (13) gives

$$p = \mathbf{P}y = \mathbf{P}\upsilon_\rho + p_i b_i, \tag{18}$$

where p_i is the ith column vector of the parity matrix $\mathbf{P}$. p_i is also called the ith channel vector, since it is related to the ith beacon. The direction of p_i, which is associated with the failed beacon, is most closely aligned to the parity vector, p. Therefore, the faulty measurement can be identified as

$$n_f = \arg\max_{i=1,\ldots,n}\frac{|p^T p_i|}{|p_i|} = \arg\max_{i=1,\ldots,n}\left(\cos\theta_i\right), \tag{19}$$

where n_f is the channel number of the faulty signal, and p_i is the ith column vector of the parity matrix $\mathbf{P}$. p_i is also called the ith channel vector since it is related to the ith beacon. At least five visible beacons are required in order to perform the failure exclusion. Figure 4 gives the plot of a parity space, in which the number of the visible beacons is assumed to be five. This figure shows five channel vectors corresponding to the five beacons shown, and the parity vector is closest to the channel vector associated with the failed beacon, which may cause the signal to fail.

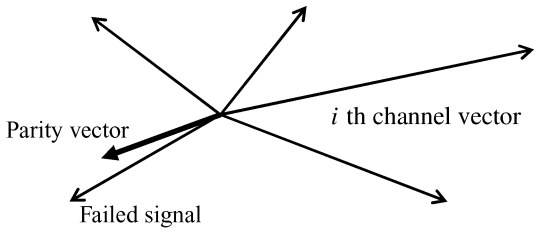

Fig. 4. Parity space plot with five channels.

7. Simulations and Experiments

7.1. Simulation of the DOP

The effectiveness the GDOP is examined for two representative cases. In the first case, the three beacons form an equilateral triangle on the X–Y plane inscribed in a circle centered on the origin of radius 1,000 distance units. The locations of the beacons are $(-500\sqrt{3}, -500, 3000)$, $(0, 1000, 3000)$, and $(-500\sqrt{3}, -500, 3000)$. The data acquisition area of the system is a square at the base plane, spanning in each direction from $-4{,}000$ to 4,000 units. In the second case, the stations are located at$(-500, -5, 3000)$, $(0, 5, 3000)$ and $(-500, -5, 3000)$, i.e., they are almost aligned along the X-axis. The acquisition area in this case is also the base plane.

Figure 5 shows the contour plots of each case. It is observed that in Case 1, the GDOP value increases as the mobile robot moves away from the center of the equilateral triangle, while in Case 2, the GDOP is much bigger when the robot is moving in an area where the three beacons are almost coplanar.

7.2. Experimental environment

The localizer, which sends out the RFID and measures the distance to the beacons, is designed in the intelligent robot laboratory using DSP TMS320C2406 processors. Four ultrasonic transmitters are designed using MSP430 devices (see Fig. 6) and C++ has been used for the system development, to support the object-oriented structural design.

7.3. Experiment of the attenuation compensation

Two experimental results are compared, to illustrate the function of the attenuation compensation, as described by Eq. (1). Four different distances are measured three times in each experiment. The results are shown in Table I, indicating that the error is increasing as the distance increases. On the other hand, after applying the attenuation compensation, the errors do not increase dramatically when the distance is increased, as is shown in Table II.

https://doi.org/10.1017/S0263574709005712 Published online by Cambridge University Press

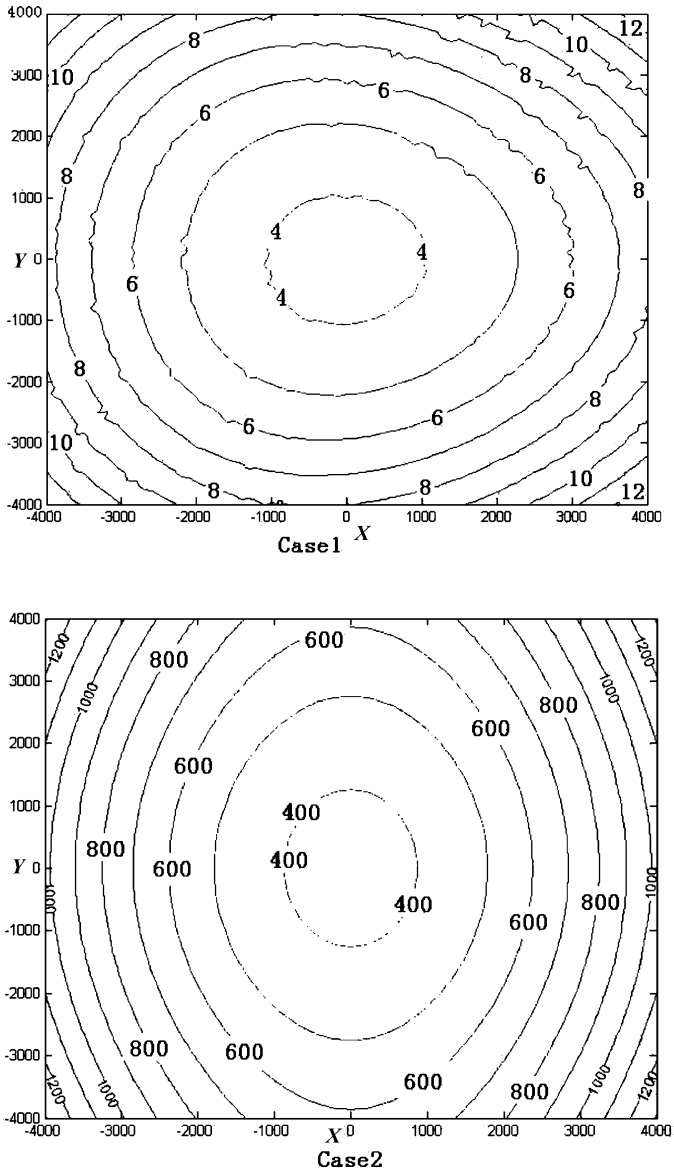

Fig. 5. Simulation of the DOP.

7.4. Experiments of DOP

Two experiments have been carried out to demonstrate the performance of the multi-block applications. Experiment A uses the traditional navigation method with three beacons, initialized by traditional auto-calibration using three seeds. The auto-calibration results, i.e., the coordinates of three beacons, and the DOP value in the auto-calibration is shown in Table III.

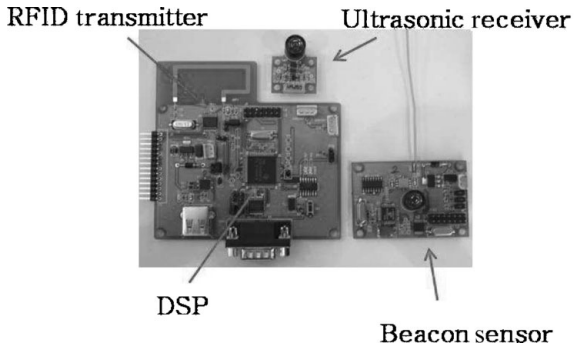

Fig. 6. The localizer and beacon sensor.

Table I. Measuring error without the attenuation compensation scheme.

Distance	Measurements			Errors		
1 m	1002	1003	1002	2	3	2
2 m	1998	2007	2005	2	7	5
3 m	3024	3031	3017	24	31	17
4 m	4033	4054	4056	33	54	56

Table II. Measuring error with the attenuation compensation scheme.

Distance	Measurements			Errors		
1 m	1002	1001	1003	2	1	3
2 m	2004	2003	2005	4	3	5
3 m	3008	3006	3006	8	6	6
4 m	4004	4008	4005	4	8	5

Experiment B uses the multi-block application method proposed in this paper. In this experiment, 5 beacons are used, which are initialized by an optimal auto-calibration method with 20 seeds. For each localization process, the five range measurements are evaluated by the signal integrity monitoring algorithm, to detect and isolate faults. Then the Beacon Selection module chooses the best three beacons to calculate the robot position using trilateration. The result of the optimal auto-calibration is shown in Table IV.

The *X*–*Y* coordinate route of the mobile robot, obtained from the two experiments, is presented for comparison in Fig. 7. As expected, the navigation result of experiment A has several faults, shown by the blue points out of the path in the figure. In experiment B, these faults are avoided, and the route is much smoother than that of experiment A. Figure 8 shows the navigational results in the *Z*-axis. As the mobile robot moves on the horizontal experiment workspace, the *Z*-axis result is actually the robot's height. In contrast, in Fig. 8, the multi-block application gives much better accuracy than the traditional method.

Table III. Beacon deployment in experiment A.

Beacon	Coordinates	GDOP	HDOP	VDOP
A	(−217, −642, 2091)	9.057	7.710	4.754
B	(2785, 4290, 2114)	21.99	12.17	18.31
C	(2959, −265, 2189)	9.922	8.596	4.955

Table IV. Beacon deployment in experiment B.

Beacon	Coordinates	GDOP	HDOP	VDOP
1	(−226, −210, 2303)	2.7543	2.3823	1.1178
2	(−61, 3967, 2348)	2.7428	2.3660	1.1572
3	(3087, 4076, 2204)	3.0365	2.4758	1.2286
4	(2904, −36, 2314)	2.6676	2.3382	1.0761
5	(1223, 1483, 2678)	2.2637	2.1522	1.6096

https://doi.org/10.1017/S0263574709005712 Published online by Cambridge University Press

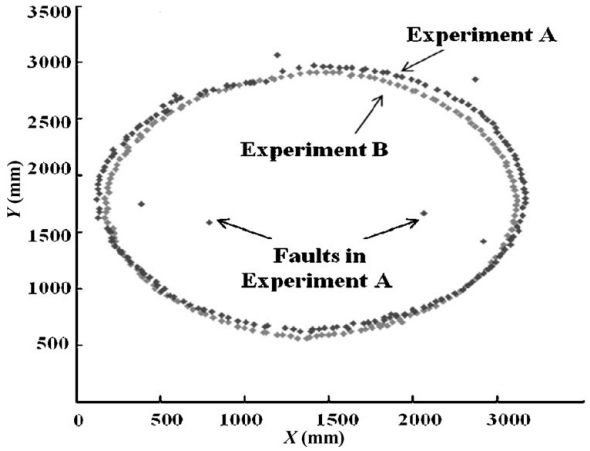

Fig. 7. Comparison of results in the X–Y plane.

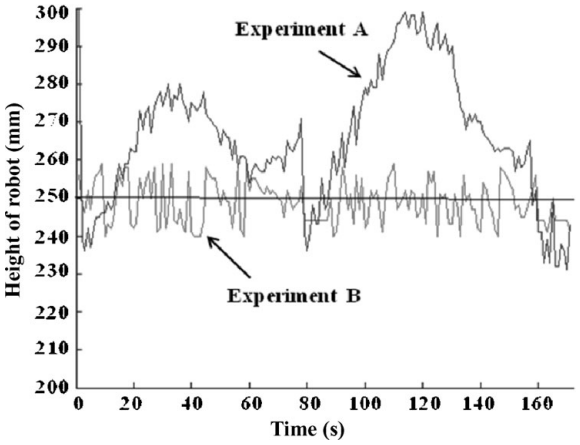

Fig. 8. Error comparison along the Z-axis.

7.5. Experiments of navigation

The deployment of the beacons and the route taken by the mobile robot are shown in Fig. 9. The workspace is divided into four blocks, A–D and thirteen beacons are deployed in the workspace with the mobile robot moving from block A to block D.

Three different experiments are implemented to prove the functions and advantages of the multi-block navigation system. Experiment 1, as shown in Fig. 10, shows the navigation without the faulty detection algorithm by performing signal integrity monitoring. A faulty beacon (beacon 5) is located in the navigation process. This results in

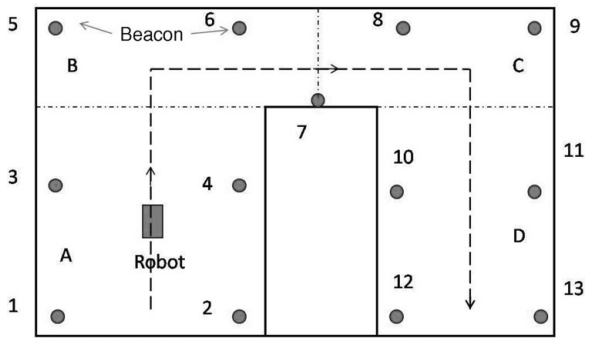

Fig. 9. The route of the mobile robot.

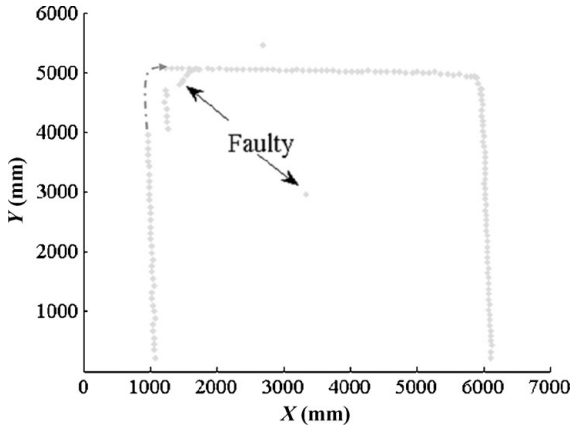

Fig. 10. Navigation without the faulty detection.

the system obtaining faulty localization results when beacon 5, of Fig. 9, is used for the navigation.

Experiment 2 is carried out without the beacon selection algorithm based on the DOP analysis. The beacons are selected according to their distances from the robot and the result is shown in Fig. 11. The navigation result is seen to have different levels of error when the beacons change, because the system did not choose the beacons on their DOP affect to the triangulation results. As a result, there were several gaps in the route of the robot when the beacons are changing.

Experiment 3 uses the multi-block navigation system proposed in this paper and the result is shown in Fig. 12. The serious faults and route gaps are avoided by the application of the signal integrity monitoring and the DOP analysis. As expected, the system obtains a smoother route for the robot and there is less error in this experiment than in experiments 1 and 2.

8. Conclusions

This paper has presented multi-block navigation of an ABS indoor localization system, for navigating mobile robots within complicated environments. The spatial identification module is used to provide the spatial information to the

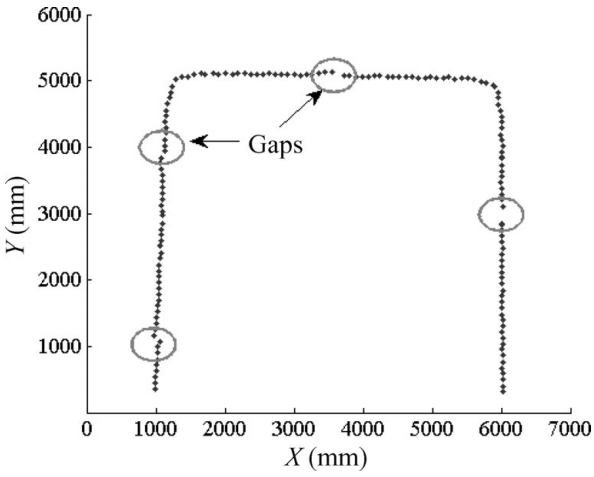

Fig. 11. Navigation without the DOP analysis.

https://doi.org/10.1017/S0263574709005712 Published online by Cambridge University Press

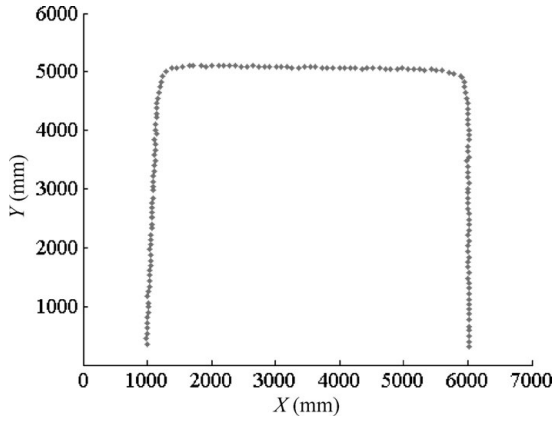

Fig. 12. Results of the multi-block navigation.

robot. The proposed attenuation compensation algorithm aims to reduce the error in the TOF measurements and a signal integrity monitoring algorithm has been introduced in order to detect and isolate faulty beacons in the navigation process. In addition, a DOP analysis process has been used to select the best beacons to ensure the least error in the triangulation calculation. Using the multi-block navigation of the ABS system, the mobile robot can move freely among the different blocks of the workspace with the ubiquitous navigation service, which includes coordinate, spatial identity, and navigation precision information.

Acknowledgments

This work was supported by the IT R&D program of MKE/IITA [2008-S033-01, Development of Global Seamless Localization Sensor].

References

1. C. Randell and H. Muller, "Low Cost Indoor Positioning System," **In**: *Ubiquitous Computing* (Springer-Verlag, Sep. 2006) pp. 42–48.
2. S. Y. Yi and B. W. Choi, "Autonomous navigation of indoor mobile robots using a global ultrasonic system," *Robotica* **22**, 369–374 (2004).
3. C. C. Tsai, "A localization system of a mobile robot by fusing dead-reckoning and ultrasonic measurements," *Trans. Instrum. Meas.* **47**(5), 1399–1404, (Oct. 1998).
4. J. P. Wang, W. F. Tian and Z. H. Jin, "Study on integrated micro inertial navigation system/GPS for land vehicles," *Intell. Trans. Syst.* **2**, 1650–1653 (2003).
5. Davide Merico and Roberto Bisiani, "Indoor Navigation with Minimal Infrastructure," *Fourth Workshop on Position, Navigation and Communication,* Hannover, Germany, 141–144, (2007).
6. J. M. Yun, S. B. Kim and J. M. Lee, "Robust Positioning a Mobile Robot with Active Beacon Sensors," *LNAI 4251, ISSN 0302-9743*, Part I, 890–897, (2006).
7. S. B. Kim and J. M. Lee, "Precise indoor localization system for a mobile robot using auto calibration algorithm," *Korean Robot. Soc.* **2**(1), 40–47 (2007).
8. Federico Thomas and Lluís Ros, "Revisiting trilateration for robot localization," *IEEE Trans. Robot.* **21**(1), 93–101, (2005).
9. D. E. Manolakis, "Efficient solution and performance analysis of 3-D position estimation by trilateration," *IEEE Trans. Aerosp. Electron. Syst.* **32**, 1239–1248 (1996).
10. M. S. Grewal and A. P. Andrews, *Kalman Filtering: Theory and Practice Using MATLAB* (Wiley, New York, 2000).
11. G. H. Golub and C. F. Van Loan, *Matrix Computations*, (The Johns Hopkins University Press, Baltimore, MD, 1996).
12. M. A. Sturza, "Navigation system integrity monitoring using redundant measurements," *J. Inst. Navig.* **35**(4), 483–501 (1988).
13. Yi-Hsueh Tsai and Fan-Ren Chang, "Using Multi-Frequency for GPS Positioning and Receiver Autonomous Integrity Monitoring," *Proceedings of the 2004 IEEE International Conference on Control Applications*, Taipei, Taiwan, (2004).
14. S. Feng and R. Ioannides *et al.*, "A measurement domain receiver autonomous integrity monitoring algorithm," *GPS Solut.* **10**, 85–96 (2006).

https://doi.org/10.1017/S0263574709005712 Published online by Cambridge University Press